CrossMark

The tropospheric biennial oscillation defined by a biennial mode of sea surface temperature and its impact on the atmospheric circulation and precipitation in the tropical eastern Indo-western Pacific region

Jinju Kim[1] · Kwang-Yul Kim[1]

Abstract Temporal and spatial patterns of anomalous atmospheric circulation and precipitation over the Indo-Pacific region are analyzed in conjunction with the Tropospheric Biennial Oscillation as represented by the biennial mode of sea surface temperature anomalies (SSTA). The biennial components of key variables are identified independently of other variability via CSEOF analysis. Then, its impact on the Asian-Australian monsoon is examined. The biennial mode exhibits a seasonally distinctive atmospheric response over the tropical eastern Indo-western Pacific (EIWP) region (90°–150°E, 20°S–20°N). In boreal summer, local meridional circulation is a distinguishing characteristic over the tropical EIWP region, whereas a meridionally expanded branch of intensified zonal circulation develops in austral summer. Temporally varying evolution and distinct timing of SSTA phase transition in the Indian and Pacific Oceans is considered a main factor for this variation of circulation in the tropical EIWP region. The impact of the biennial mode is not the same between the two seasons, with different impacts over ocean areas in Asian monsoon and Australian monsoon regions.

✉ Kwang-Yul Kim
kwang56@gmail.com; kwang56@snu.ac.kr

1 School of Earth and Environmental Sciences, Seoul National University, Seoul 08826, Republic of Korea

1 Introduction

Bulk of tropical SSTA variability can be explained in terms of low-frequency variability associated with the Northern Pacific decadal oscillations, (quasi) biennial variability (Rasmusson et al. 1990; Barnett 1991; Kim 2002; Clarke et al. 1998) and global warming (Yeo and Kim 2014). A significant fraction of ENSO variability is explained as an irregular interplay of these nearly independent physical mechanisms (see Fig. 8 in Yeo and Kim 2014). In addition to the effect of tropical SST increase due to global warming, the low-frequency mode, as the name implies, describes ENSO variability on decadal time scales. The quasi-biennial variability, a prominent feature in the tropical Indian and Pacific Oceans, is an important element for understanding the tropospheric biennial oscillation (TBO) mechanism (Meehl et al. 2003).

TBO is known as an ocean-atmosphere coupled system across the Indian and Pacific Oceans, which involves changes in pressure, precipitation, sea surface temperature (SST) and wind (Meehl 1987, 1997; Kim and Lau 2001; Loschnigg et al. 2003). The TBO system exerts a strong influence on the local monsoons over Asia and Australia (Chang and Li 2000; Chung et al. 2011; Li et al. 2001, 2006, 2013; Liu et al. 2014; Meehl 1997; Meehl and Arblaster 2002; Shen and Lau 1995; Pillai and Mohankumar 2008; Wang et al. 2008; Webster et al. 1998; Wu and Kirtman 2004). Therefore, elucidation of the TBO mechanism is important in understanding monsoon variability. Many studies have been carried out to expound the mechanism of this ocean-atmospheric coupled system in association with the regional monsoons and quasi-biennial SSTA variability. Meehl (1987, 1997), Meehl and Arblaster (2002) and Meehl et al. (2003) reported that the southeastward migration of the convection center during
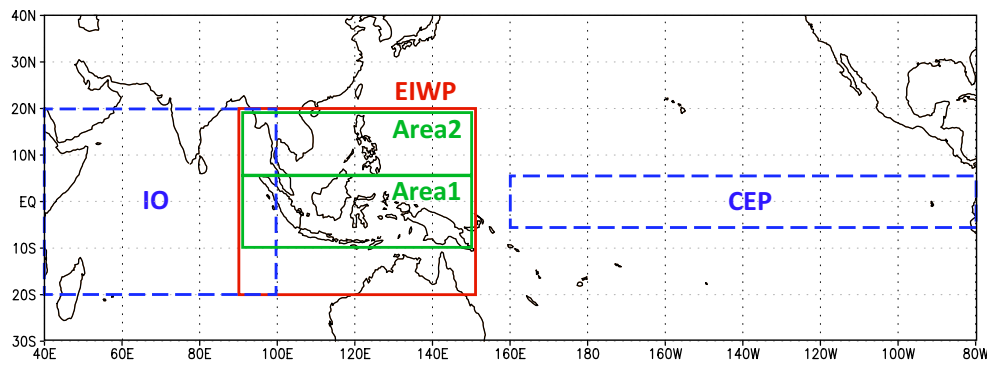
Fig. 1 The main focus area is the *red box* (90°–150°E, 20°S–20°N), and is called the tropical eastern Indian-western Pacific (EIWP) region in the present study. *Green boxes* represent the equatorial (Area1: 90°–150°E, 10°S–6°N) and northern (Area2: 90°–150°E, 6°–20°N) branches of the meridional circulation in boreal sum-mer. *Blue boxes* represent the tropical Indian Ocean (40°–110E, 20°S–20°N) and the tropical central/eastern Pacific (160°E–80°W, 6°–6°N), where the evolution of SSTA affects the meridional circulation in the EIWP region in boreal summer

the evolution of the Indian-Australian monsoon ties the Pacific and Indian Oceans and is a main factor for the system's 2-year fluctuation. Wang et al. (2001) and Liu et al. (2013) elaborated that the biennial tendency in the tropical Pacific induces anomalous cyclone/anticyclone over the western North Pacific, thereby modulating the East Asian summer monsoon. On the other hand, it was also suggested that local SSTA over the Indo-Pacific warm pool interacting with the western North Pacific Subtropical High could produce 2–3 year variability (Chung et al. 2011; Li et al. 2006; Sui et al. 2007).

The biennial variability of local summer precipitations has been studied frequently over East Asia and the western North Pacific (Shen and Lau 1995; Li et al. 2006, 2013; Chung et al. 2011; Liu et al. 2013, 2014) and South Asia and India (Li et al. 2001; Pillai and Mohankumar 2008; Wu and Kirtman 2004). Despite that local monsoons are constantly changing in time and space, monsoon systems are usually treated as stationary in many studies. Although relatively rare, some studies regard the Asian (Indian)-Australian monsoon as a seasonally migrating system (Chang and Li 2000; Meehl 1997; Meehl and Arblaster 2002; Wang et al. 2008). In many studies, however, the biennial variability is explained in the presence of strong seasonal variability (i.e., the seasonal cycle). In the presence of a dominant physical mechanism with a distinct spatio-temporal evolution (i.e., the seasonal cycle), an accurate interpretation of the intrinsic evolution feature and physical mechanism of the biennial mode is much hampered. Further, the seasonally and hemispherically distinct impact of the biennial mode is yet to be delineated in a rigorous manner.

In present study, detailed evolution features of the biennial mode are examined to understand its physical mechanism. The spatial and temporal change of SSTA and the ensuing evolution and transition of atmospheric fields through the biennial coupling of the Indian and Pacific Oceans are dealt with explicitly. It is also investigated in what manner and to what extent the biennial mode impacts the Asian-Australian monsoon precipitation. Identifying factors influencing the local monsoons is also crucial in understanding the global monsoon system, which represents the global-scale variation of the three-dimensional atmospheric circulation and corresponding precipitation change (An et al. 2014; Trenberth et al. 2000; Wang 2009; Wang et al. 2014).

CSEOF analysis is carried out to separate the seasonal cycle and biennial mode from other variability. The main focus area (Fig. 1) is the tropical eastern Indo-western Pacific (EIWP) region (90°–150°E, 20°S–20°N), since the biennial variability is prominent and the seasonal migration of the Asian-Australian monsoon system is developed in this region. Also atmospheric variability in this region is known to exert significant impacts on the monsoonal flow and summer precipitation in both hemispheres.

Data and methods used in this study are introduced in Sect. 2. In Sect. 3, results based on CSEOF analysis are discussed. The evolution patterns of the biennial mode during a 2-year period and the seasonal cycle of precipitation are described in detail, and the physical relationship among different variables is analyzed. Finally, concluding remarks are presented in Sect. 4.

2 Data and method of analysis

2.1 Data

Monthly Extended Reconstruction Sea Surface Temperature (ERSST) version 3 dataset for 103 years (1910–2012) is used in the present study; the ERSST dataset covers the

near-global region (0°–360°E, 46°S–60°N). In order to understand the evolutions of atmospheric variables, the Twentieth Century Reanalysis (20CR) version 2 (Compo et al. 2011) monthly datasets both at the surface and 17 pressure levels (1000–200 hPa) for the same period of time are utilized in the present study. We also used the ECMWF's atmospheric reanalysis of the twentieth century (ERA-20C) (Poli et al. 2013) to confirm the results produced from the 20CR dataset.

2.2 CSEOF analysis

The seasonal cycle and the biennial oscillation mode are extracted from the ERSST dataset using cyclostationary EOF (CSEOF) analysis (Kim et al. 1996; Kim and North 1997). This separation is best accomplished by using a long SST record as in Yeo and Kim (2014). In CSEOF analysis, spatio-temporal data are decomposed into CSEOF loading vectors (CSLVs), $B_n(r, t)$, and principle component (PC) time series, $T_n(t)$:

$$Data(r, t) = \Sigma_n B_n(r, t) T_n(t). \tag{1}$$

In this study, CSLV for each mode consists of 24 monthly spatial patterns evolving in time (nested period = 24 months). The first mode ($n = 1$) of the ERSST dataset represents the seasonal cycle of SST and the fourth mode ($n = 4$) denotes the biennial oscillation signal (Yeo and Kim 2014), which describes the transition from the La Niña phase to the El Niño phase in the Pacific Ocean over a 2-year period. The resulting pattern is not overly sensitive to the length of record or domain size. The corresponding PC time series describes longer-term variability of the biennial mode and explains how the intensity of the biennial signal has changed in the record. CSEOF analysis is also conducted on others atmospheric variables with the same nested period (24 months).

2.3 Regression analysis in CSEOF space

The target variable in this study is SST. A multivariate regression analysis in CSEOF space (Kim et al. 2015) is carried out to identify the variation of atmospheric variables pertaining to the SST seasonal cycle mode and the biennial oscillation mode. The regression analysis is written as

$$T_n^{sst}(t) = \Sigma_{m=1}^M \alpha_m^{(n)} T_m^{atm}(t) + \varepsilon^{(n)}(t), \tag{2}$$

where $T_n^{sst}(t)$ is the nth PC time series of the SST (target variable), $T_m^{atm}(t)$ is the mth PC time series of an atmospheric variable (predictor variable), $\{\alpha_m^{(n)}\}$ are the regression coefficients, $\varepsilon^{(n)}(t)$ is regression error time series, and M is the number of predictor PC time series used for regression. The regressed CSLV of an atmospheric variable, which

is physically consistent with the SST evolution of the nth CSEOF mode, can be obtained via

$$B_n^{reg}(r, t) = \Sigma_{m=1}^M \alpha_m^{(n)} B_m^{atm}(r, t), \tag{3}$$

where $B_m^{atm}(r, t)$ are the original CSLVs of the predictor variable. With the regression analysis in CSEOF space, entire data collection can be rewritten as follows:

$$Data(r, t) = \Sigma_n \{ SST_n(r, t), \ SLP_n^{reg}(r, t),$$
$$UV_n^{reg}(r, t), \ P_n^{reg}(r, t), \cdots \} T_n^{sst}(t), \tag{4}$$

where $\{SST_n(r, t), SLP_n^{reg}(r, t), UV_n^{reg}(r, t), P_n^{reg}(r, t), \cdots\}$ are the loading vectors of the target and predictor variables; they share the PC time series, $T_n^{sst}(t)$, of the target variable.

3 Results

3.1 Nested period of analysis

In earlier studies, spectral analysis has often been used to identify the quasi-biennial signal in the precipitation data. Many studies conclude that there is no rigorous 2-year periodicity in the precipitation data. While the TBO is frequently seen as a quasi-biennial oscillation, its phase is strongly locked to the calendar months. Thus, the assumption of the 2-year periodicity seems reasonable. Further, evidence of a biennial component of monsoon precipitation has been presented (e.g. Meehl and Arblaster 2011). Figure 2a shows the AR spectra of the 15–36 month bandpass filtered and domain-averaged precipitation time series. The time series averaged over the northern (90°–150°E, 5°–20°N) and southern (100°–150°E, 20°–5°S) tropical regions both exhibit conspicuous spectral peaks at approximately 2.3, 1.7, and 1.4 years. Figure 2b shows the AR spectra of the biennial mode PC time series identified from the SSTA and also the domain-averaged precipitation in the northern and southern regions. As can be seen in the figure, the spectral content of the PC time series of the domain-averaged precipitation time series is similar to that of the SSTA biennial mode even without any regression analysis in CSEOF space. The AR spectra of the PC time series exhibit two major spectral peaks at ~11.4 and ~4.8 years. These are the spectral peaks of the amplitude time series modulating the biennial oscillation with a 2-year period. As a result of the modulation, we expect peaks at

$$\omega_1 = \omega_b + \omega_a \quad \text{and} \quad \omega_2 = \omega_b - \omega_a, \tag{5}$$

where ω_1 and ω_2 are the two new frequencies generated from the frequency ω_a of the PC time series modulating the biennial frequency ω_b ($\omega_b = 0.5$ year^{-1}). It can be easily verified that the periods corresponding to (ω_1, ω_2) are approximately 1.7 and 2.4 years for the modulation period
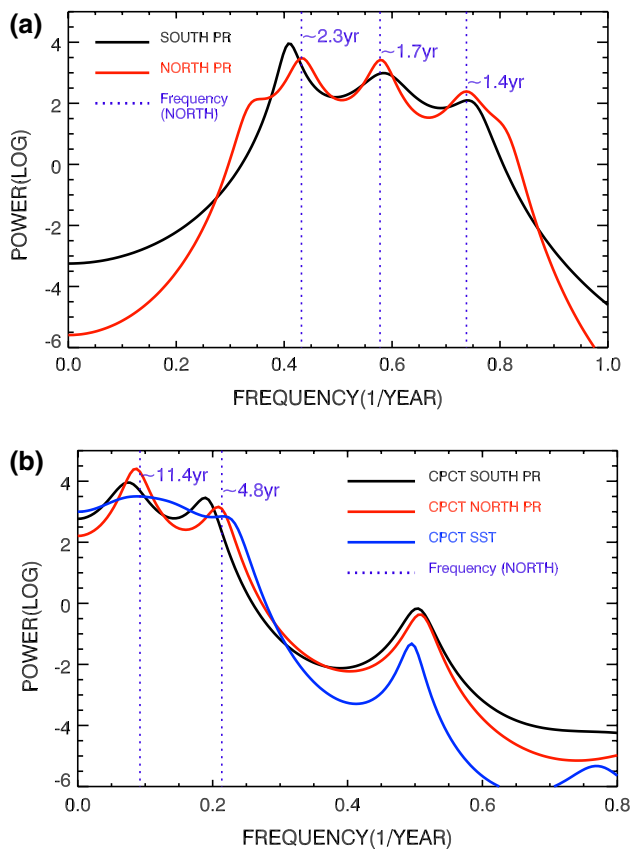
Fig. 2 Auto-regressive spectral density of **a** the area-averaged precipitation anomaly over the northern (90°–150°E, 5°–20°N) and southern tropical region (100°–150°E, 20°–5°S) after 15–36 month band-pass filtering, and **b** the PC time series of precipitation for the biennial mode of SSTA and those of the precipitation averaged over the northern and southern regions

of 11.4 years and are approximately 1.4 and 3.4 years for the modulation period of 4.8 years. Figure 2a shows the three of these peaks clearly with the peak corresponding to the longest period (3.4 years) is missing; the longest peak is missing, since the time series was high-passed filtered with a cutoff frequency of 3 years. Judging from the fact that SSTA associated with the biennial mode is strongly phase-locked to the calendar months, it is reasonable to assume the biennial mode with a 2-year periodicity. The quasi-biennial periodicity seems to result from the modulation of the 2-year periodicity. In this sense, the biennial mode in the present study is the oceanic manifestation of the TBO and represent the same physical mechanism (Meehl and Arblaster 2011).

3.2 Biennial mode of sea surface temperature

The biennial component of variability in the near global SST (0°–360°E, 46°S–60°N) is extracted via CSEOF analysis. The biennial signal is extracted as the fourth CSEOF

mode and explains about 9 % of the total variance aside from the seasonal cycle. In the tropical Pacific (120°–280°E, 30°S–30°N), this mode explains ~20 % of the total SSTA variability, and its impact on the Asian-Australian monsoon should be much more substantial than the percent variance it explains. As discussed in Yeo and Kim (2014), the biennial mode of SST, a prominent evolution feature in the tropics, is one of the primary mechanisms of ENSO variability together with the low-frequency variability mode and the global warming mode.

Figure 3 depicts the seasonal patterns of the 2-year loading vector of the biennial mode. In this study, we will call the period from May of the first year to April of the second year the cold phase and from May of the second year to April of the first year the warm phase. The seasonal evolution patterns depict the development of the warm and cold phases of SSTA and the phase transition between them. During the mature phase, well-developed El Niño or La Niña patterns are seen in the tropical Pacific. The delayed action oscillator (Suarez and Schopf 1988; Battisti and Hirst 1989) and the recharge-discharge oscillator (Jin 1997a, b) are suggested as the fundamental physical mechanism for the transition and oscillation of the biennial mode. For the sake of brevity, atmospheric response to the cold phase of SSTA will be addressed below. In the warm phase, the patterns are nearly opposite to those of the cold phase. Because of the irregular occurrences of the biennial mode, asymmetry between El Niño and La Niña patterns may have been smeared; this is an important caveat in the present study.

Negative SSTA begins to emerge in the tropical eastern Pacific Ocean in May (Fig. 3a), while SSTA over the tropical Indian Ocean and western Pacific remains to be positive. This negative SSTA over the eastern Pacific extends toward the central Pacific in July–September and the warm SSTA dwindles toward the east in the Indian Ocean. When the cold phase matures with strong negative SSTA over the central-eastern Pacific, triple anomaly patterns are observed from the Indian Ocean to the Pacific Ocean with a horseshoe-shaped positive SSTA over the western Pacific between the basin-wide cold anomalies in the Indian and central-eastern Pacific Oceans. After negative SSTA reaches a maximum over the tropical Pacific in December, SSTA over the Indian Ocean peaks during January–March. Subsequently, positive SSTA develops in the tropical eastern Pacific in the following May as the cold phase decays. It should be mentioned that the timing of the phase transition is different between the tropical Pacific Ocean (boreal spring) and the tropical Indian Ocean (boreal autumn). These evolution patterns are similar to those for the TBO derived from composite analyses based on Indian monsoon strength (e.g. Meehl 1997; Meehl et al. 2003) thus confirming these earlier studies with a more sophisticated statistical analysis. Also a quasi-biennial periodicity was assumed in earlier studies (Barnett
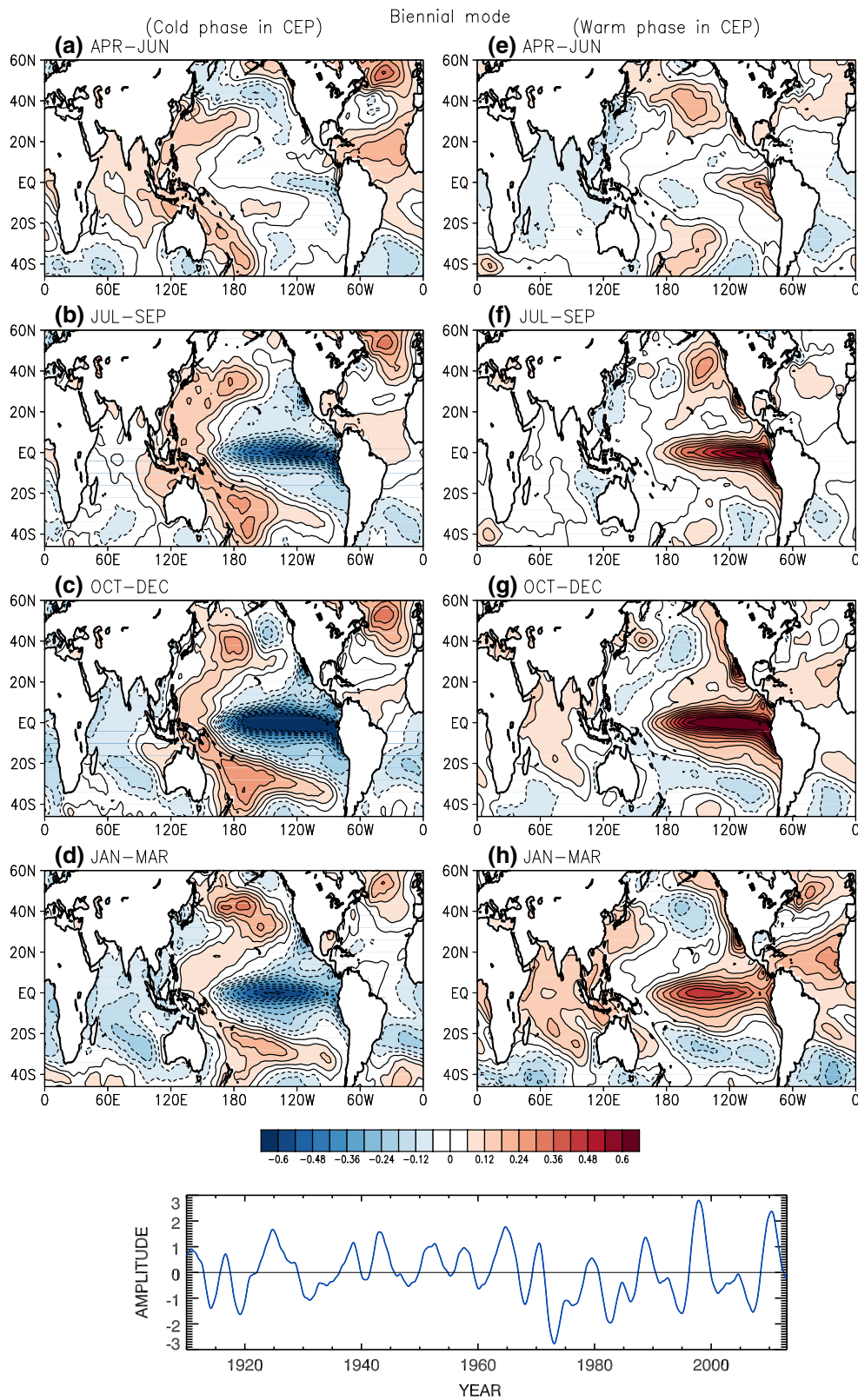
Fig. 3 (*Top*) The seasonal patterns of the CSEOF loading vector of the biennial mode derived from the near-global (0°–360°E, 46°S–60°N) sea surface temperature and (*bottom*) the corresponding PC time series
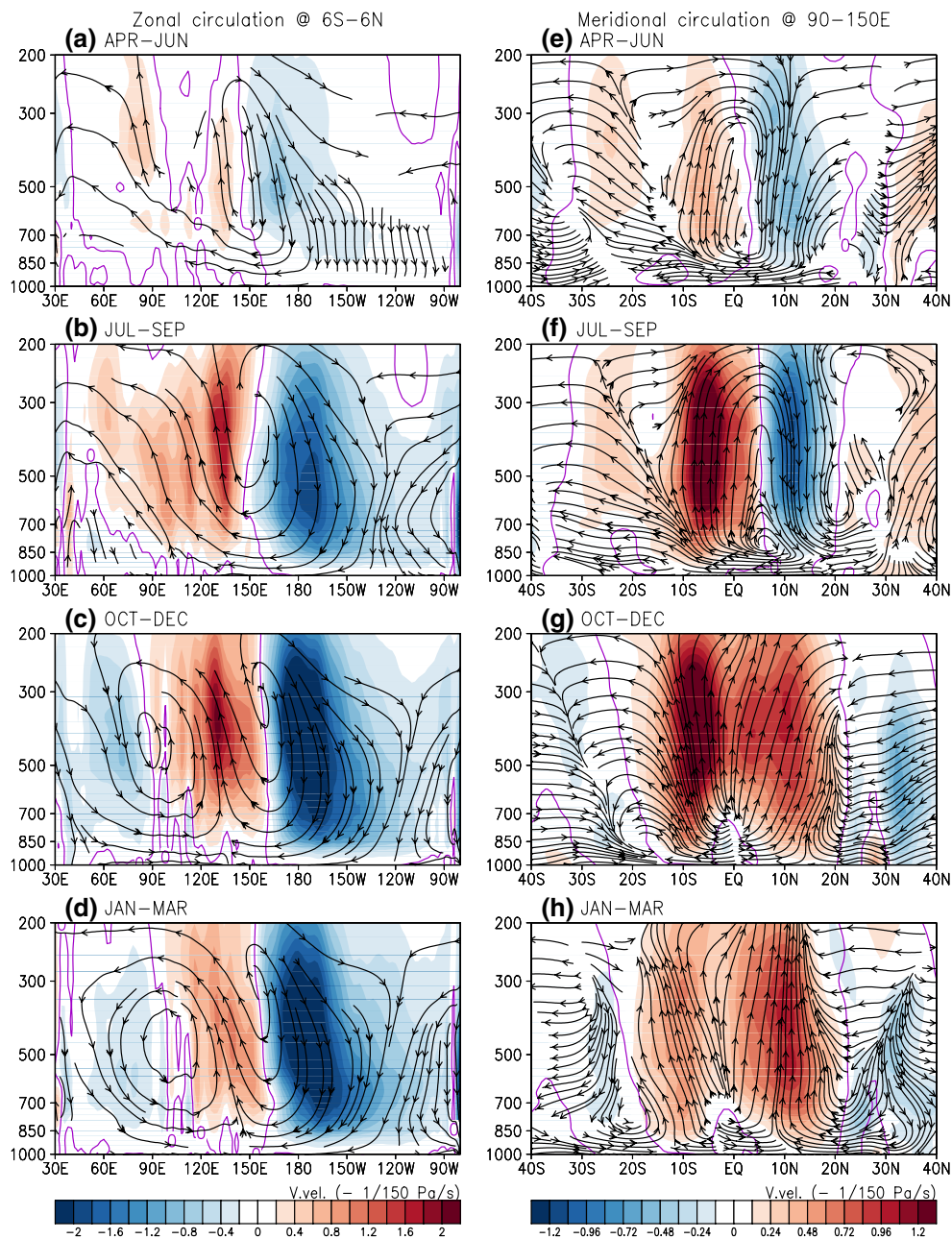
Fig. 4 Seasonal evolution patterns of the zonal circulation in the latitude band of 6°S–6°N (*left panels*), and the meridional circulation in the zonal band of 90°–150°E (*right panels*) for the cold phase of the

biennial mode. *Shading* denotes the vertical velocity ($-pa\ s^{-1}$). During the positive phase of the biennial mode, the situation reverses

1991; Li et al. 2006; Chung et al. 2011). The PC time series in the bottom panel of Fig. 3 shows the long-term amplitude variation of the biennial mode.

3.3 Seasonal evolution of atmospheric circulation in the biennial mode

The SSTA change in the tropical region for the biennial mode directly influences the equatorial zonal circulation,

which exhibits a seasonal link with the local meridional circulation in the tropical EIWP region. Figure 4 depicts the seasonal evolution of the equatorial zonal circulation and the local (90°–150°E longitudinal average) meridional circulation during the cold phase of the biennial mode. In the equatorial region, the atmospheric change is nearly concurrent with the local SSTA evolution.

In boreal spring, descending motion develops with the negative SSTA in the central-eastern Pacific. Meanwhile,
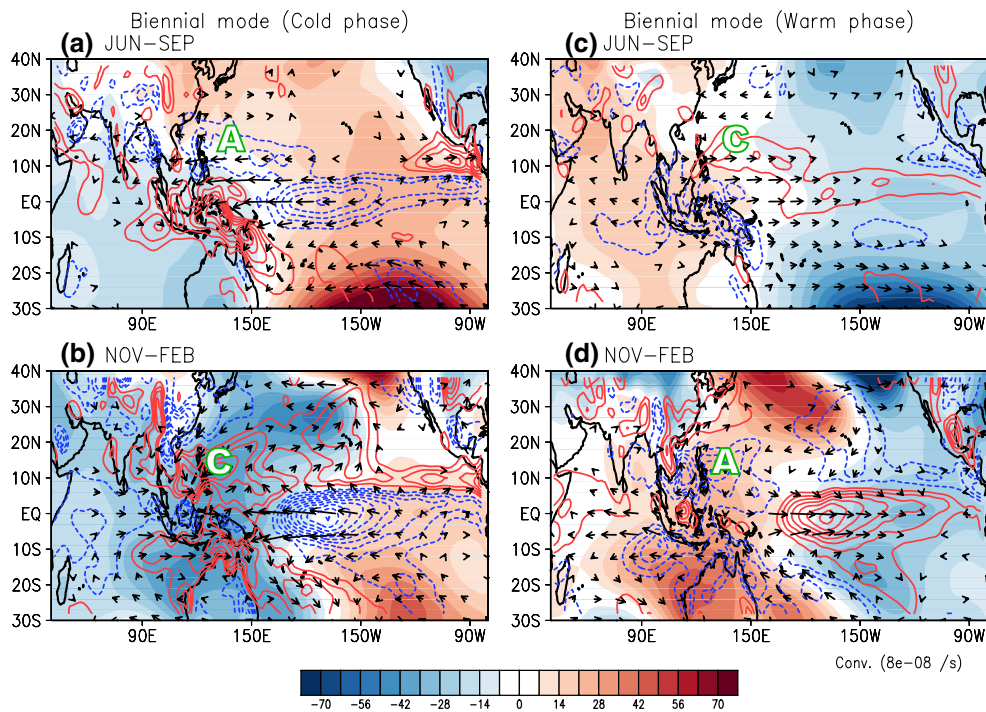
Fig. 5 The 4-month averaged low-level (1000–850 hPa) horizontal wind (*vector*), horizontal wind convergence (*contour*; 8×10^{-8} s^{-1}), and SLPA (*shading*) associated with the biennial mode for boreal summer (*upper panels*) and austral summer (*lower panels*)

ascending motion also develops over the Indian Ocean and the far-western Pacific with warm SSTA and enhances with the intensification of the cold SSTA in the central-eastern Pacific. The anomalous convection induces the low-level westerly over the tropical Indian Ocean and cold water emerges from the western coast (Figs. 3b, 4b). Downward motion appears over the western Indian Ocean in late summer and expands toward the eastern Indian Ocean during boreal fall and winter as the cold SSTA in the equatorial Pacific reaches a maximum. Simultaneously, the strengthened upward motion migrates slightly eastward and shrinks over the western Pacific. This upward motion induces low-level easterly over the equatorial Pacific and westerly over the equatorial Indian Ocean. After the mature phase in the central-eastern Pacific, the equatorial vertical motion generally begins to weaken.

In the local meridional circulation within the 90°–150°E zonal band, an asymmetry is remarkable with a northward shift of the circulation center during boreal spring and summer (Fig. 4e, f; Chung et al. 2011; Wu et al. 2009), while a broad rising motion occurs in the tropics during boreal fall and winter (Fig. 4g, h). The anomalous convection is observed continuously over the equatorial region, which is related to the equatorial zonal circulation. Anomalous downward motion over the northern tropical region (~10°–20°N) has persisted from the previous fall until summer without any sign change. During spring and summer,

therefore, local meridional circulation is well observed in the tropical EIWP region. In boreal fall, this meridional circulation is replaced by a north–south expanded branch of the zonal circulation when the vertical motion switches a sign in the northern tropics (Fig. 4g).

This seasonally distinctive feature is also seen in the low-level horizontal circulation. Figure 5 represents the low-level pressure and circulation patterns for boreal summer (May–September) and austral summer (November–February). In boreal summer of the cold phase (Fig. 5a), the temperature contrast between the tropical Pacific Ocean and tropical Indian Ocean induces anomalous high over the tropical Pacific and anomalous low over the tropical Indian Ocean. In accordance with this anomalous pressure pattern, anomalous easterly develops over the tropical Pacific. It converges over the Maritime Continent with weak equatorial westerly in the eastern Indian Ocean and diverges in the northern tropics with southeasterly along the southwestern periphery of the anticyclonic circulation over the western North Pacific. This is consistent with the formation of the Indian Ocean dipole as part of the TBO noted by Loschnigg et al. (2003) and seen in Fig. 3c. As can be seen in Fig. 4e, f, the vertical motion and low-level convergence/divergence are connected through the local meridional circulation.

In austral summer (Fig. 5b), a noticeable difference from boreal summer is the intensification of the anomalous low and its expansion to the western Pacific. Cyclonic

circulation is established on both sides of the equator in the tropical EIWP region (the western North Pacific and Australia). It looks similar to the development of the anticyclonic/cyclonic circulation over the western North Pacific during El Niño/La Niña events (Wang et al. 2000; Wang and Zhang 2002). Also westerly wind anomalies appear in the tropical eastern Indian Ocean with westerly anomalies extending to the western equatorial Pacific. Such wind anomalies would be conducive to triggering downwelling equatorial Kelvin waves that would act to lower the thermocline in the eastern equatorial Pacific, thus contributing to a subsequent transition of SST anomalies from negative to positive in northern spring in Fig. 3e (also shown by Meehl et al. 2003). A combination of the tropical zonal wind and the cyclonic circulations in both hemispheres encourages the development of low-level wind convergence over the tropical EIWP. It is physically consistent with the upward motion over the tropical EIWP. This explains the expanded zonal circulation with strengthened downward motion centered at ~180°E.

In the warm phase (Fig. 5c, d), the responses are nearly opposite. Due to development of warm SSTA over the central-eastern Pacific, anomalous low is over the Pacific and anomalous high over the Indian Ocean generally. In austral summer of the warm phase, anomalous high expands toward the western Pacific and strengthens.

3.4 Role of different timings of SSTA evolutions in the Indian and Pacific Oceans

It is emphasized that the atmospheric circulation over the Indo-Pacific region due to the biennial oscillation of SSTA varies significantly from boreal summer to austral summer. In boreal summer, the local meridional circulation is conspicuous over the tropical EIWP region (Fig. 4f), whereas the tropical zonal circulation is strengthened and meridionally widened in austral summer (Fig. 4c, g). A plausible explanation for this difference is in the relative size and intensity of the central and eastern Pacific SSTA and the different timing of SSTA phase transition over the Pacific and the Indian Oceans.

In boreal summer, SSTA over the central-eastern Pacific is not wide and strong enough to exert influence in the whole tropics of the EIWP region (Fig. 3b); atmospheric variables respond directly to SSTA in the oceanic EIWP region. Therefore anomalous convection occurs near the Maritime Continent and over India, with suppressed convection over the Bay of Bengal and Philippine Sea regions since the remote SSTA forcing is confined near the equator. In austral summer, on the other hand, a remote forcing of maximum SSTA and the subsequent new SSTA of the same sign over the Indian Ocean influence broader tropics via strengthened zonal circulation (Fig. 4g, h).
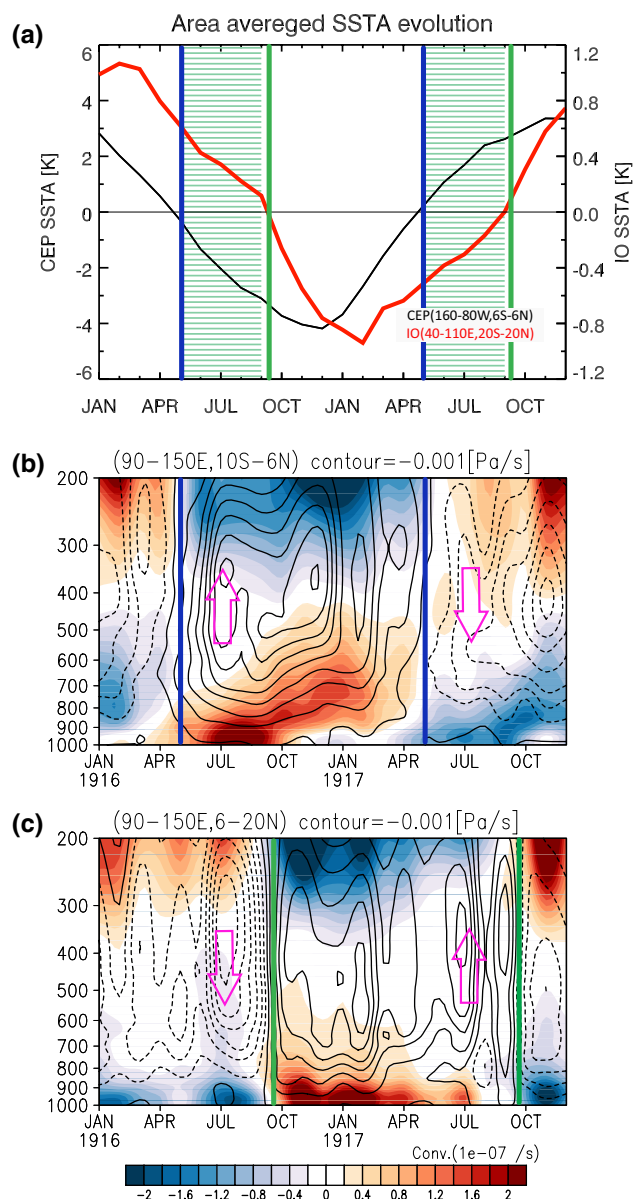

Fig. 6 a Time evolution of area-averaged SSTA over (*black*) the central eastern Pacific (160°–80°W, 6°S–6°N) and (*red*) Indian Ocean (30°–110°E, 20°S–20°N). *Green shading* indicate the time gap of their phase transition. **b** Horizontal wind convergence/divergence (*shading*) and vertical velocity (*contour*) in the 10°S–6°N vertical section, and **c** for the 6°–20°N section

A combination of SSTA over both the tropical Pacific and Indian Oceans is important to explain the atmospheric response over the tropical EIWP region. Figure 6a shows that the new phase of the basin-wide SSTA over the Pacific Ocean appears in May (blue lines) and that over the Indian Ocean appears later in September–October (green lines). Due to the different timing of the phase transition between the two oceans, SSTA of opposite signs are observed over the tropical oceans for boreal summer (green striped region

in Fig. 6a; see also Fig. 3): one sign over the central-eastern Pacific and the opposite sign over the western Pacific and the Indian Ocean. During austral summer, SSTA over the Indian Ocean and that over the central-eastern Pacific are of identical sign separated by the SSTA of opposite sign in the far western Pacific. This change of SSTA relocates the anomalous pressure pattern accordingly, accompanied by a noticeable change in the low-level circulation over the tropical EIWP region (Fig. 5a, b).

Figure 6b, c shows the temporal evolution of the anomalous horizontal convergence/divergence and vertical motion in the equatorial band (10°S–6°N; Area1 in Fig. 1) and the northern tropical latitudes (6°–20°N; Area2 in Fig. 1) respectively over the EIWP region (90°–150°E, 20°S–20°N) in the biennial mode. A set of low-level wind convergence (divergence) and upper-level wind divergence (convergence) is dynamically coherent with the ascending (descending) motion. Near the equator (Fig. 6b), change in the horizontal convergence and vertical motion is coincident with the phase transition of the central-eastern Pacific SSTA (blue lines). In the northern tropical oceanic region (Fig. 6c), change in the horizontal convergence and vertical motion is tied with the transition of the Indian Ocean SSTA (green lines). In boreal summer of the cold phase (first striped interval in Fig. 6a), the sign of the atmospheric response over the equatorial Maritime Continent is reversed with the emergence of the cold SSTA over the central-eastern Pacific, which promotes anomalous high over the Pacific Ocean and anomalous low in the tropical Indian Ocean. On the other hand, low-level wind divergence and downward motion continues in the northern tropical oceanic region since the remote forcing of SSTA over the central-eastern Pacific is confined to the narrow equatorial region. The downward motion in the northern tropical ocean region is, in fact, strengthened by the convection over the equatorial Maritime Continent (Chung et al. 2011; Wu et al. 2009). As a consequence, local meridional circulation is developed over the tropical EIWP region. Meanwhile, the anomalous high over the western North Pacific produces southeasterly diverging from the equatorial easterly in the EIWP region; this also strengthens the low-level divergence in the EIWP region. This anticyclonic circulation may be explained as the Kelvin wave type response to the basin-wide warming in the Indian Ocean, which has lingered from the previous fall (Wu et al. 2009, 2010; Yuan et al. 2012; Yang et al. 2007; Xie et al. 2009).

When the warm SSTA changes to cold SSTA in the tropical Indian Ocean (after the transition interval), the atmospheric variables reverse their signs in the northern tropical ocean region. Therefore, low-level convergence and upward motion is observed over the entire tropical EIWP. The associated cyclonic circulation looks similar to the Rossby wave response (Gill 1980; Taschetto et al. 2010; Yuan et al.

2012; Wang et al. 2000; Wu and Kirtman 2004) to the local (western Pacific) warming and intensified remote forcing by the central-eastern Pacific and Indian cooling.

3.5 Moisture flux and precipitation in the biennial mode

The biennial mode will have impact on the variability of the Asian-Australian monsoon system, which is essentially the seasonal migration of precipitation between the two hemispheres. The fact that the circulation over the tropical EIWP region varies seasonally with the biennial oscillation of SSTA means that the Asian-Australian monsoon precipitation is perturbed by seasonally varying atmospheric circulation.

Figure 7 shows the seasonal cycle of precipitation over the Indo-Pacific region. Precipitation begins to increase above the annual mean value in May/June in the northern hemisphere with a maximum in August. Precipitation dwindles in October over the northern hemispheric continental areas. As the precipitation band crosses the equator, monsoon precipitation increases above the annual mean value in the southern hemisphere in December. This seasonal excursion of precipitation depicts the evolution of the Asian-Australian monsoon system. It is noteworthy that there is a strong asymmetry in the precipitation patterns between the two hemispheres primarily because of the very distinct land-sea configurations. The corresponding PC time series shows that the amplitude of the seasonal cycle has fluctuated by about ±20 % during the data period. The intensity of the Asian (Australian) monsoon seasonal precipitation has varied as shown by the corresponding PC time series.

The anomalous low-level circulation induced by the biennial mode alters moisture transport. Considering that the seasonal cycle and the biennial mode of SSTA both influence the temporal evolution of moisture and wind, anomalous moisture flux is calculated from

$$q\vec{u} - \overline{q\vec{u}} = \left(\overline{q} + q'\right)\left(\overline{\vec{u}} + \vec{u}'\right) - \overline{\left(\overline{q} - q'\right)\left(\overline{\vec{u}} + \vec{u}'\right)}$$
$$= \overline{q}\vec{u}' + q'\overline{\vec{u}} + q'\vec{u}' - \overline{q'\vec{u}'}, \tag{6}$$

where $\overline{q}$ and $\overline{\vec{u}}$ represent the climatology (the seasonal cycle) of moisture and wind, while q' and $\vec{u}'$ denote anomalous moisture and wind induced by the biennial mode. Then, the convergence of anomalous moisture flux is given by $-\nabla \cdot \left(\overline{q}\vec{u}' + q'\overline{\vec{u}} + q'\vec{u}' - \overline{q'\vec{u}'}\right)$.

Figure 8 describes the anomalous moisture flux, moisture convergence and precipitation due to the SSTA biennial oscillation in the summer of each hemisphere during the cold phase. The first term in (6) explains the majority of moisture convergence in the lower troposphere, which
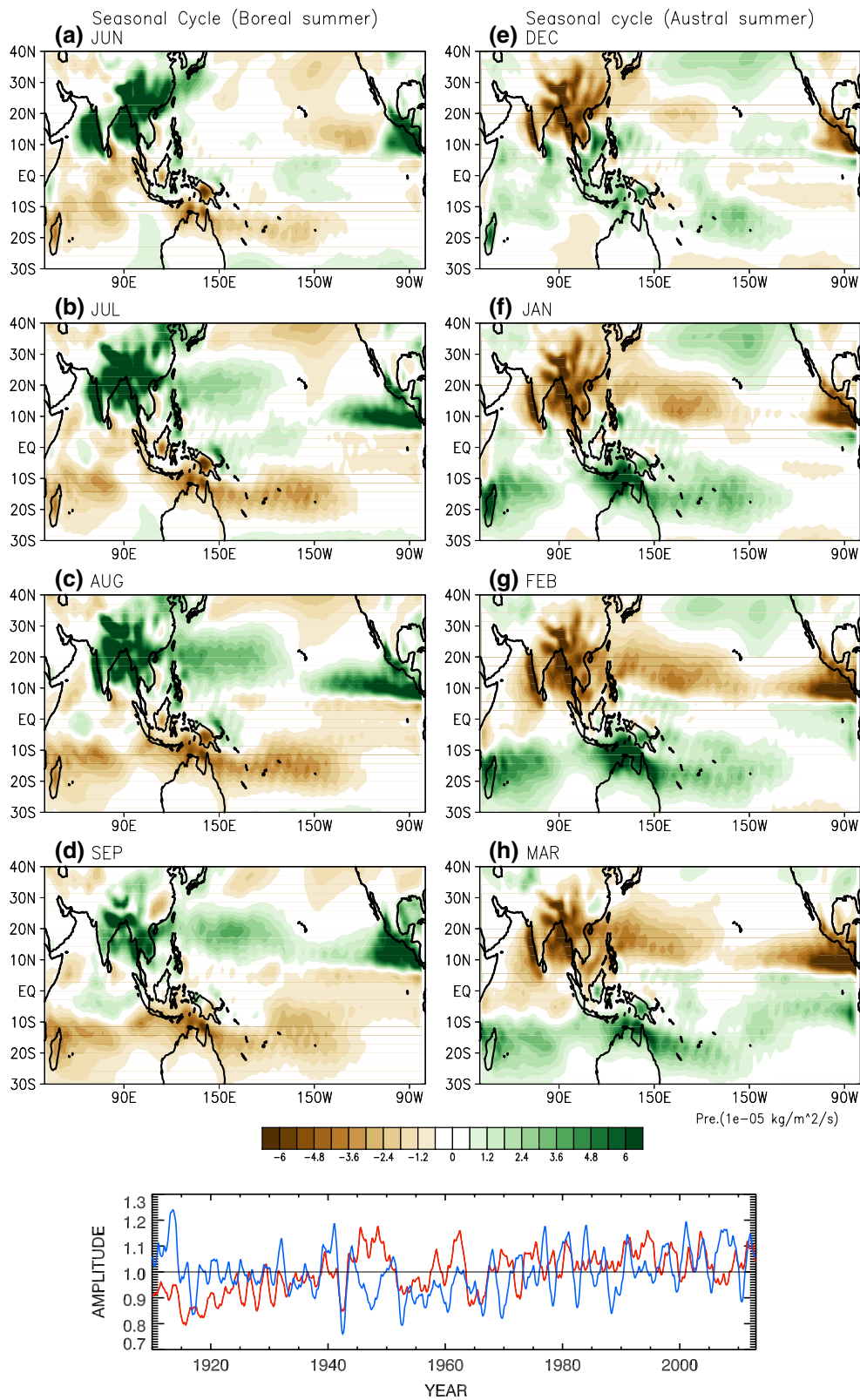
Fig. 7 (*Top*) The seasonal patterns of precipitation over the Indo-Pacific region and (*bottom*) the corresponding PC time series. The *left column* depicts the Asian Monsoon (*red* PC time series) and the *right column* the Australian Monsoon (*blue* PC time series)
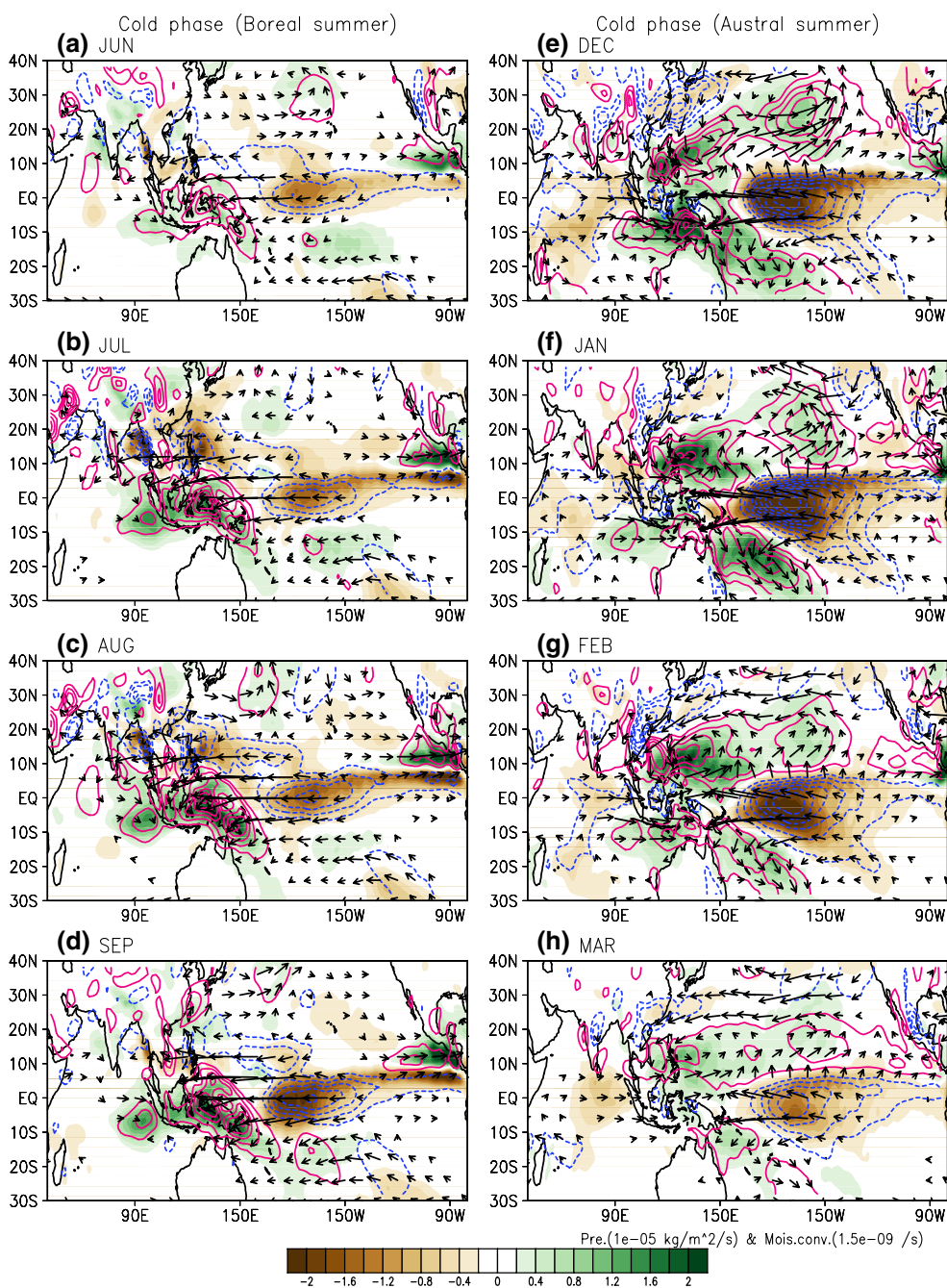
Fig. 8 Anomalous moisture flux (*vector*), moisture convergence (*contour*; 1.5×10^{-9} s^{-1}) and precipitation rate (*shading*) for the cold phase of the biennial mode during boreal summer (June–September) and austral summer (December–March)

implies that the variation of low-level wind is more crucial than that of specific humidity in explaining the anomalous moisture transport associated with the biennial oscillation of SSTA (Wu and Kirtman 2004). The influence of the biennial mode is relatively weaker in higher latitudes than in the tropics. The anomalous precipitation, particularly in the tropics, highly resembles the anomalous moisture convergence and also the anomalous vertical motion (figure not shown). This means that the change in moisture convergence accompanied by vertical motion is the primary mechanism of the variation in the precipitation rate. This biennial variability in the precipitation rate within the zonal band of 90°–150°E explains about 9 and 11 % of the total variance aside from the seasonal cycle in the northern and southern tropical regions, respectively.

In boreal summer, the descending branch of anomalous meridional circulation and the low-level moisture divergence in the northern tropical EIWP region induces a dry condition over the ocean regions of the Bay of Bengal, the Philippine Sea and the Indochina Peninsula, while there is above normal precipitation over India (Fig. 8a–c). Anomalous anticyclonic circulation in the subtropical western North Pacific supplies moisture to the central and eastern parts of China. In austral summer, negative precipitation anomaly over the northern tropical ocean region disappears and positive precipitation anomaly in the equatorial region extends to the whole tropics in the 110°–160°E zonal band including the northern part of Australia (Fig. 8e–g; Meehl 1997; Meehl and Arblaster 2002; Meehl et al. 2003). This wet condition is linked to the upward branch of the enhanced and enlarged zonal circulation with low-level moisture convergence due to the intensified negative SSTA forcing over the tropical Pacific.

To understand the impact of the biennial mode on the Asian-Australian monsoon system in a precise manner, the biennial mode should be considered together with the seasonal cycle in Fig. 7. In boreal summer of the cold phase, when the seasonal cycle of precipitation band resides in the northern hemisphere (Fig. 7a–d), Asian monsoon precipitation decreases over the Indochina peninsula and ocean areas in the Bay of Bengal, South China Sea and the Philippine Sea (Fig. 8a–d). On the other hand, monsoon precipitation increases over India and in eastern and central China since the intensified southwesterly from the anomalous anticyclonic circulation over the western North Pacific transports more moisture to the continent (Xie et al. 2009; Yang et al. 2007; Wu et al. 2009). In austral summer of the cold phase, when the seasonal precipitation band lies in the southern hemisphere (Fig. 7e–h), the positive precipitation anomaly over the northern part of Australia makes the monsoon precipitation stronger and also the onset of the Australian rainy season earlier (Fig. 8e–h).

As is evident in Fig. 8, the impact of the biennial mode is dramatically different between the two hemispheres, since both the SSTA and the ensuing atmospheric circulation differ significantly during the rainy seasons in the two hemispheres. Some studies (Chang and Li 2000; Meehl et al. 2003; Meehl and Arblaster 2002; Yu et al. 2003) show that the biennial changes in the Indian monsoon precipitation and the ensuing Australian monsoon precipitation are of the same sign. In the present study, the sign of anomalous precipitation over the Indian continental region is the same as that over Australia, but is opposite over the ocean areas of the Bay of Bengal, South China and Philippine Seas. In general, the biennial contribution of SSTA to the Asian monsoon in the Bay of Bengal, the Indochina peninsula, the South China Sea and the Philippine Sea is achieved via the local meridional circulation, whereas its

contribution to the Australian monsoon is through the tropical zonal circulation.

4 Summary and concluding remarks

It was scrutinized how atmospheric variables evolve in time and space in association with the TBO as characterized by the biennial mode of SSTA. The biennial mode is separated from the seasonal cycle and the other internal variability (e.g. low-frequency variability of ENSO discussed in Yeo and Kim 2014) via CSEOF and regression analysis. In addition, it was investigated how the biennial mode exerts impacts on the Asian-Australian monsoon precipitation, which represents the seasonal cycle of precipitation with a distinct spatio-temporal evolution from that of the biennial mode.

The SSTA evolution associated with the biennial mode exhibits not only a strong seasonality but also a delicate difference in timing in the tropical Pacific and the Indian Oceans. As a result, atmospheric circulation over the tropical EIWP region changes significantly from boreal summer to austral summer. In boreal summer, the local meridional circulation is prominent in the tropical EIWP region, whereas the strengthened tropical zonal circulation is more dominant in austral summer. A fundamental reason for this difference is that the tropical EIWP region is affected in a subtle way by SSTA both in the Pacific and the Indian Oceans. The intensity and size of SSTA over the central-eastern Pacific Ocean and the timing of SSTA transition in the Pacific and the Indian Oceans are considered as key factors for the meticulous circulation change in the tropical EIWP region. As a result, the effect of the biennial mode in the monsoon precipitation differs significantly between the two hemispheres.

Figure 9 depicts a simple schematic of the circulation and SSTA change during the cold phase of the biennial mode. During JJAS, relatively narrow and weak SSTA over the central-eastern Pacific and the residual SSTA over the tropical Indian Ocean induce air-sea interaction via the equatorial zonal circulation and the local (90°–150°E) meridional circulation. The northern branch (6°–20°N) of the local meridional circulation is linked to the low-level anticyclonic circulation arising from the anomalous high over the western North Pacific. Accordingly, the downward motion and low-level moisture divergence in the northern tropical ocean region accompanies the negative precipitation anomaly during boreal summer. The effect of zonal circulation is important in boreal summer. In fact, the upward branch of the zonal circulation in the 90°–150°E band is instrumental for the development of the meridional circulation. During NDJF, relatively wide and strong SSTA over the central-eastern Pacific and the new phase of the basin-wide SSTA over the tropical Indian Ocean result in air-sea interaction via the intensified zonal circulation.
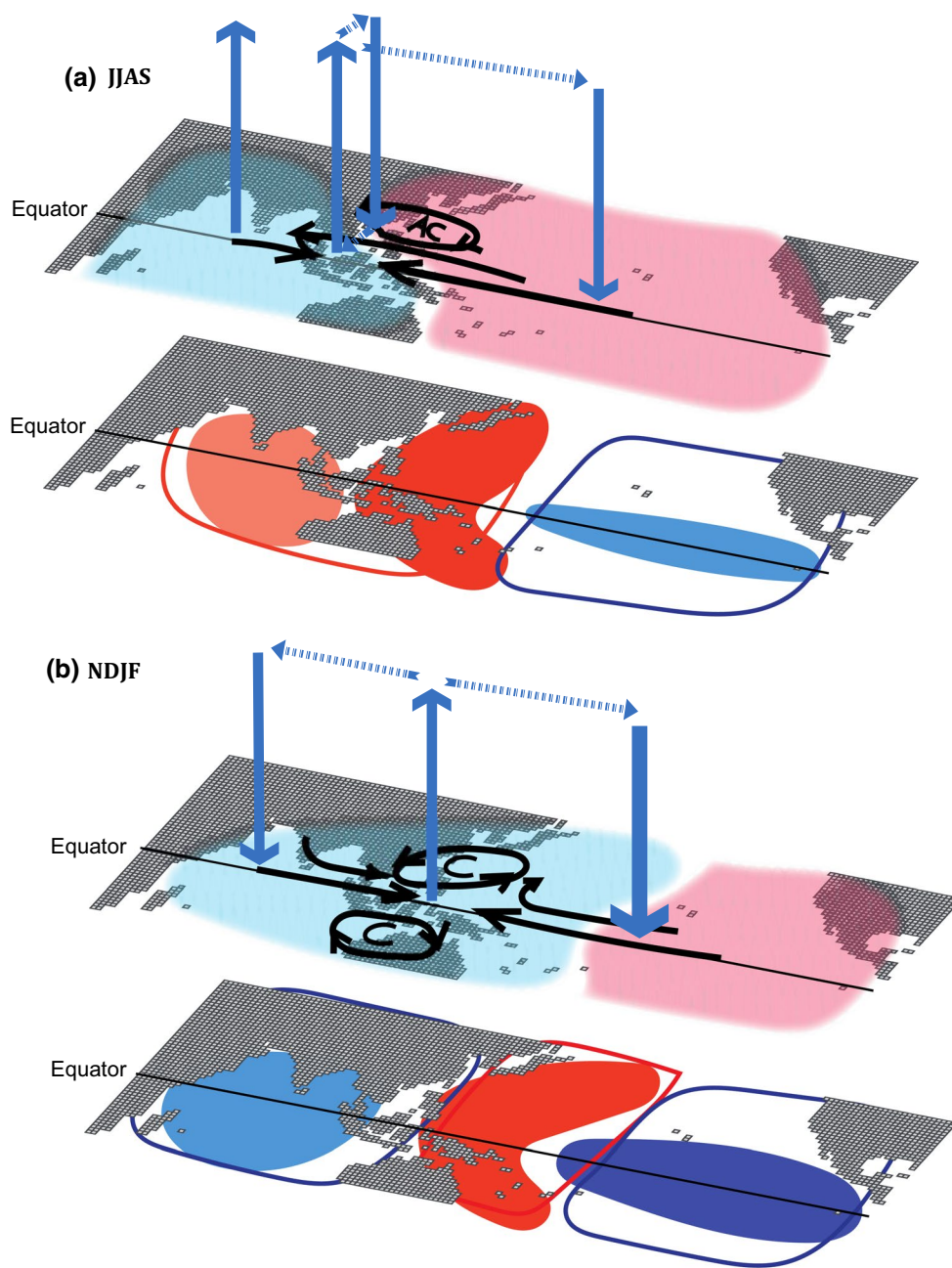
Fig. 9 Schematic diagram of circulation (*upper*) and SSTA (*lower*) change in the cold phase of the biennial mode in **a** JJAS and **b** NDJF. (*upper panel*) *Pink shading* indicates anomalous high and *light blue shading* indicates anomalous low. *Blue vectors* denote vertical circu-

lation and upper-level wind. *Black arrows* represent anomalous low-level horizontal circulation. (*Lower panel*) *Red shading* means warm SSTA and *blue shading* cold SSTA. *Orange* (*cyan*) implies that SSTA is weaker than that for *red* (*blue*)

To the north and south of the upward branch of the zonal circulation, low-level cyclonic circulation develops as a Rossby wave-type response to the warming in the western Pacific. The ensuing SLPA pattern also helps the development of the low-level cyclonic circulations. The upward motion and low-level moisture convergence in the southern tropics, henceforth, produces positive precipitation anomaly during austral summer. During the cold phase,

therefore, precipitation is reduced over the oceanic area in the northern tropics, and it is increased with an earlier onset of monsoon in Australia. In the warm phase, the situation reverses. It should be noted that there exists strong asymmetries in the two hemispheres, not only because of the seasonal variation of SSTA in the tropics but also because of the different atmospheric responses arising from the SSTA forcing.

References

An Z et al (2014) Global monsoon dynamics and climate change. Annu Rev Earth Planet Sci. doi:10.1146/annurev-earth-060313-054623

Barnett TP (1991) The interaction of multiple time scales in the tropical climate system. J Clim 4:269–285

Battisti DS, Hirst AC (1989) Interannual variability in a tropical atmosphere-ocean model: influence of the basic state, ocean geometry, and nonlinearity. J Atmos Sci 46:1687–1712

Chang CP, Li T (2000) A theory for the tropical tropospheric biennial oscillation. J Atmos Sci 57:2209–2224

Chung PH, Sui CH, Li T (2011) Interannual relationship between the tropical sea surface temperature and summertime subtropical anticyclone over the western North Pacific. J Geophys Res 116:D13. doi:10.1029/2010JD015554

Clarke AJ, Liu X, Gorder SV (1998) Dynamics of the biennial oscillation in the equatorial indian and far western Pacific Oceans. J Clim 11:987–1001

Compo GP et al (2011) The twentieth century reanalysis project. Q J R Meteorol Soc 137:1–28

Gill AE (1980) Some simple solutions for heat-induced tropical circulation. Q J R Meteorol Soc 106:447–462

Jin FF (1997a) An equatorial ocean recharge paradigm for ENSO. Part I: conceptual model. J Atmos Sci 54:811–829

Jin FF (1997b) An equatorial ocean recharge paradigm for ENSO. Part II: a stripped-down coupled model. J Atmos Sci 54:830–847

Kim KY (2002) Investigation of ENSO variability using cyclostationary EOFs of observational data. Meteorol Atmos Phys 81:149–168

Kim KM, Lau KM (2001) Dynamics of monsoon-induced biennial variability in ENSO. Geophys Res Lett 28:315–318

Kim KY, North GR (1997) EOFs of harmonizable cyclostationary processes. J Atmos Sci 54:2416–2427

Kim KY, North GR, Huang J (1996) EOFs of one-dimensional cyclostationary time series: computations, examples, and stochastic modeling. J Atmos Sci 53:1007–1017

Kim KY, Benjamin H, Na H (2015) Theoretical foundation of cyclostationary EOF analysis for geophysical and climatic variables: concepts and examples. Earth Sci Rev 150:201–218. doi:10.1016/j.earscirev.2015.06.003

Li T, Zhang Y, Chang CP, Wang B (2001) On the relationship between Indian Ocean sea surface temperature and Asian summer monsoon. Geophys Res Lett 28:2843–2846

Li T, Liu P, Fu X, Wang B, Meehl GA (2006) Spatiotemporal structures and mechanisms of the tropospheric biennial oscillation in the Indo-Pacific Warm Ocean regions. J Clim 19:3070–3087

Li Y, Li J, Feng J (2013) Boreal summer convection oscillation over the Indo-Western Pacific and its relationship with the East Asian summer monsoon. Atmos Sci Lett 14:66–71

Liu Y, Ding YH, Gao H, Li W (2013) Tropospheric biennial oscillation of the western Pacific subtropical high and its relationships with the tropical SST and atmospheric circulation anomalies. Chin Sci Bull 58:364–3672

Liu Y, Hu ZZ, Kumar A, Peng P, Collins DC, Jha B (2014) Tropospheric biennial oscillation of summer monsoon rainfall over East Asia and its association with ENSO. Clim Dyn. doi:10.1007/s00382-014-2429-5

Loschnigg J, Meehl GA, Webster PJ, Arblaster JM, Compo GP (2003) The Asian monsoon, the tropospheric biennial oscillation and the Indian Ocean Dipole in the NCAR CSM. J Clim 16:2138–2158

Meehl GA (1987) The annual cycle and interannual variability in the tropical Pacific and Indian Ocean region. Mon Weather Rev 115:27–50

Meehl GA (1997) The South Asian monsoon and tropospheric biennial oscillation. J Clim 10:1921–1943

Meehl GA, Arblaster JM (2002) The tropospheric biennial oscillation and Asian-Australian monsoon rainfall. J Clim 15:722–744

Meehl GA, Arblaster JM (2011) Decadal variability of Asian-Australian monsoon-ENSO-TBO relationships. J Clim 24:4925–4940

Meehl GA, Arblaster JM, Loschnigg J (2003) Coupled ocean-atmosphere dynamical processes in the tropical Indian and Pacific Ocean regions and the TBO. J Clim 16:2138–2158

Pillai PA, Mohankumar K (2008) Local Hadley circulation over the Asian monsoon region associated with the tropospheric Biennial Oscillation. Theor Appl Climatol 91:171–179

Poli P, et al (2013) The data assimilations system and initial performance evaluation of the ECMWF pilot reanalysis of the 20th century assimilating surface observations only (ERA-20c). ERA Rep Ser 14 [http://www.ecmwf.int/publications]

Rasmusson EM, Wang X, Ropelewski CF (1990) The biennial component of ENSO variability. J Clim 5:594–614

Shen S, Lau KM (1995) Biennial oscillation associated with the East Asian summer monsoon and tropical sea surface temperatures. J Meteorol Soc Japan 73:105–124

Suarez MJ, Schopf PS (1988) A delayed action oscillator for ENSO. J Atmos Sci 45:3283–3287

Sui CH, Chung PH, Li T (2007) Interannual and interdecadal variability of the summertime western North Pacific subtropical high. Geophys Res Lett 34:L11701. doi:10.1029/2006GL029204

Taschetto AS, Haarsma RJ, Gupta AS, Ummenhofer CC, Hill KJ, England MH (2010) Australian monsoon variability driven by a Gill-Matsuno-type response to central west Pacific Warming. J Clim 23:4717–4736

Trenberth KE, Stepaniak DP, Caron JM (2000) The global monsoon as seen through the divergent atmospheric circulation. J Clim 13:3969–3993

Wang P (2009) Global monsoon in a geological perspective. Chin Sci Bull 54:1–24

Wang B, Zhang Q (2002) Pacific-East Asian teleconnection. Part II: how the Philippine Sea anomalous anticyclone is established during El Niño development. J Clim 15:3252–3265

Wang B, Wu R, Fu X (2000) Pacific-East Asian teleconnection: how does ENSO affect East Asian climate? J Clim 13:1517–1536

Wang B, Wu R, Lau KM (2001) Interannual variability of the Asian summer monsoon: contrasts between the Indian and the Western North Pacific-East Asian Monsoons. J Clim 14:4073–4090

Wang B, Yang J, Zhou T, Wang B (2008) Interdecadal changes in the major modes of Asian-Australian monsoon variability: strengthening relationship with ENSO since the late 1970s*. J Clim 21:1771–1789

Wang P, Wang B, Cheng H, Fasullo J, Guo ZT, Kiefer T, Liu ZY (2014) The global monsoon across timescales: coherent variability of regional monsoons. Clim Past 10:2007–2052

Webster PJ, Magaña VO, Palmer TN, Thomas RA, Yanai M, Yasunari T (1998) Monsoons: processes, predictability, and the prospects for prediction. J Geophys Res 103:14451–14510

Wu R, Kirtman BP (2004) The tropospheric biennial oscillation of the monsoon-ENSO system in an interactive ensemble coupled GCM. J Clim 17:1623–1640

Wu B, Zhou T, Li T (2009) Seasonally evolving dominant interannual variability modes of East Asian climate. J Clim 22:2992–3005

Wu B, Li T, Zhou T (2010) Relative contribution of the Indian Ocean and local SST anomalies to the maintenance of the Western North Pacific anomalous anticyclone during the El Niño decaying summer. J Clim 23:2974–2986

Xie SP, Jan H, Hiroki T, Yan D, Sampe T, Hu K, Huang G (2009) Indian Ocean capacitor effect on Indo-Western Pacific climate during the summer following El Niño. J Clim 22:2992–3005

Yang JL, Li QY, Xie SP, Liu ZY, Wu LX (2007) Impact of the Indian Ocean SST basin mode on the Asian summer monsoon. Geophys Res Lett. doi:10.1029/2006GL028571

Yeo SR, Kim KY (2014) Global warming, low-frequency variability and biennial oscillation: an attempt to understand the physical mechanisms. Clim Dyn 43:771–786

Yu JY, Weng SP, Farrara JD (2003) Ocean roles in the TBO transitions of the Indian-Australian monsoon system. J Clim 16:3072–3080

Yuan Y, Yang S, Zhang Z (2012) Different evolutions of the Philippine Sea anticyclone between the eastern and central Pacific El Niño: possible effects of Indian Ocean SST. J Clim 25:7867–7883